RESEARCH PAPER

Acute effects of short-chain alkylglycerols on blood-brain barrier properties of cultured brain endothelial cells

P Hülper[1], S Veszelka[2], F R Walter[2], H Wolburg[3], P Fallier-Becker[3], J Piontek[4]*, I E Blasig[4], M Lakomek[1], W Kugler[1] and M A Deli[2]

[1]*Department of Pediatrics I, University Medical Center Göttingen, Göttingen, Germany,* [2]*Laboratory of Molecular Neurobiology, Institute of Biophysics, Biological Research Center, Hungarian Academy of Sciences, Szeged, Hungary,* [3]*Institute of Pathology and Neuropathology, Department of General Pathology, University of Tübingen, Tübingen, Germany, and* [4]*Institute of Molecular Pharmacology, Berlin, Germany*

BACKGROUND AND PURPOSE

The blood-brain barrier (BBB) restricts drug penetration to the brain preventing effective treatment of patients suffering from brain tumours. Intra-arterial injection of short-chain alkylglycerols (AGs) opens the BBB and increases delivery of molecules to rodent brain parenchyma *in vivo*. The mechanism underlying AG-mediated modification of BBB permeability is still unknown. Here, we have tested the effects of AGs on barrier properties of cultured brain microvascular endothelial cells.

EXPERIMENTAL APPROACH

The effects of two AGs, 1-*O*-pentylglycerol and 2-*O*-hexyldiglycerol were examined using an *in vitro* BBB model consisting of primary cultures of rat brain endothelial cells, co-cultured with rat cerebral glial cells. Integrity of the paracellular, tight junction-based, permeation route was analysed by functional assays, immunostaining for junctional proteins, freeze-fracture electron microscopy, and analysis of claudin-claudin *trans*-interactions.

KEY RESULTS

AG treatment (5 min) reversibly reduced transendothelial electrical resistance and increased BBB permeability for fluorescein accompanied by changes in cell morphology and immunostaining for claudin-5 and β-catenin. These short-term changes were not accompanied by alterations of inter-endothelial tight junction strand complexity or the *trans*-interaction of claudin-5.

CONCLUSION AND IMPLICATIONS

AG-mediated increase in brain endothelial paracellular permeability was short, reversible and did not affect tight junction strand complexity. Redistribution of junctional proteins and alterations in the cell shape indicate the involvement of the cytoskeleton in the action of AGs. These data confirm the results from *in vivo* studies in rodents characterizing AGs as adjuvants that transiently open the BBB.

Abbreviations

AG, alkylglycerol; BBB, blood-brain barrier; BECs, brain endothelial cells; CPT-cAMP, 8-(4-chlorophenylthio)adenosine-3',5‰-cyclic monophosphate; EBA, Evans blue-labelled albumin; HG, 2-*O*-hexyldiglycerol; MTX, methotrexate; P_e, transendothelial permeability coefficient; PG, 1-*O*-pentylglycerol; PS_e, permeability surface area for endothelial monolayers; Ro 20-1724, 4-(3-butoxy-4-methoxyphenyl)methyl-2-imidazolidone; SF, sodium fluorescein; TEER, transendothelial electrical resistance; Tx-100, Triton X-100 detergent; YFP, yellow fluorescent protein; ZO-1, *zonula occludens* protein-1

Introduction

The blood-brain barrier (BBB) selectively regulates both trans-cellular and paracellular passage of molecules and cells between the blood and the CNS, thus impeding the treatment of brain disorders such as malignant brain tumours. In these closely associated areas between brain endothelial cells (BECs), specific structures called *zonulae occludentes* or tight junctions are expressed, whose membranes attach each other to form a virtually impermeable barrier, thus greatly hindering paracellular diffusion of hydrophilic substances through the vessel wall (Reese and Karnovsky, 1967).

Tight junctions are transmembrane complexes composed of protein polymers which form a branching network of sealing strands. Each strand is formed by a row of transmembrane proteins embedded in both plasma membranes, with extracellular domains interacting with tight junction proteins of the neighbouring cell by claudin-claudin *trans*-interactions (Blasig *et al.*, 2006). Claudin-claudin interactions are responsible for strand building of the tight junction complexes (Furuse *et al.*, 1998) and paracellular tightening (Piehl *et al.*, 2010). *Zonulae adhaerentes* or adherens junctions form a weaker barrier (Rubin and Staddon, 1999). The primary component of adherens junctions is the Ca^{2+}-regulated vascular endothelial protein, cadherin, which mediates cell-cell adhesion (Dejana *et al.*, 2008). Another set of proteins, the catenins, link the cadherins to the cytoskeleton. Proper establishment of adherens junctions is required for the expression of claudin-5 and thus they may be regulators of vascular permeability (Taddei *et al.*, 2008).

In addition to the restricted paracellular transport, transcellular transport of substances and cells into and out of the brain compartment is also very limited at the BBB because there are only a few pinocytic vesicles. The barrier functions lead to a very high transendothelial electrical resistance (TEER). In general, passage across the BBB is inversely related to the size, i.e., molecular weight, and the aqueous solubility of the compound (Pardridge, 2002). Therefore, increasing the lipophilicity of drugs has been used as one way of improving transcellular passage through the endothelial cells (Reardon *et al.*, 2006). However, many compounds that are able to penetrate the BEC membrane are very effectively transported back into the capillary lumen by efflux transporters, such as P-glycoprotein and multidrug resistance proteins, that are localized primarily at the luminal side of BECs (Golden and Pollack, 2003; Kemper *et al.*, 2004). This efflux system has generated another possibility of increasing the passage of drugs into to the brain, by inhibiting the efflux transporters. Thus, inhibition of P-glycoprotein results in increased brain penetration and slower brain elimination of those drugs which are substrates for P-glycoprotein (Fellner *et al.*, 2002; van Vliet *et al.*, 2010; O'Brien *et al.*, 2012). Other options for improved drug delivery to the CNS are to couple drugs to endogenous ligands of receptor- and carrier-mediated transport pathways, such as angiopep-2 (Demeule *et al.*, 2008) or glucosamine (Dhanikula *et al.*, 2008; see Deli, 2011). Despite intensive research, no optimal solution has yet been found for the treatment of CNS cancers, either primary tumours or metastases. The currently available cytostatic drugs are either too large (high MW) or too water-soluble to enter the brain through the blood vessel wall in sufficient concentrations or they are substrates for P-glycoprotein (Deli, 2011).

Thus, a potential approach to enhance drug delivery across biological barriers is the use of tight junction modulators to open the epithelial or endothelial paracellular route (see Deli, 2009). One previously described method of increasing the paracellular diffusion rates of molecules across brain capillaries into the brain parenchyma is the i.a. infusion of a hyperosmolar (1.37 M) mannitol solution (Neuwelt *et al.*, 1985) which opens the inter-endothelial tight junctions, via Src kinase-mediated phosphorylation of the adherens junction protein, β-catenin (Rapoport, 2000; Farkas *et al.*, 2005). Osmotic BBB disruption has already been employed in animal models and in patients with malignant brain tumours, in order to improve the effectiveness of chemotherapy (Doolittle *et al.*, 2000). However, in clinical practice, osmotic BBB opening was poorly reproducible, as it required a mannitol threshold concentration with a low therapeutic window and the opening persisted for about 6 h (Siegal *et al.*, 2000). This duration of effect may induce toxic effects of the increased BBB permeability. Moreover, this method needs interventional radiology and, up to now, its application has been restricted to a few clinics.

The ability of short-chain alkylglycerols (AGs) to increase BBB permeability have been known for more than 25 years (Unger *et al.*, 1985). In rodents, i.a. injection of AGs led to a concentration-dependent enrichment of co-administered cytostatic drugs and antibiotics in the ipsilateral hemisphere (Erdlenbruch *et al.*, 2000). In glioma-bearing rats, AGs opened the BBB in the tumour tissue and the surrounding brain (Erdlenbruch *et al.*, 2003a). Two AG derivatives, 1-*O*-pentylglycerol (PG) and 2-*O*-hexyldiglycerol (HG), have demonstrated good therapeutic range and effectiveness. After a bolus injection of PG (800 µL, 50 mM) simultaneously given with 5 mg·kg^{-1} methotrexate (MTX) into the right internal carotid artery of rats about 1.2 pmol MTX per mg brain was found in the ipsilateral hemisphere. In the contralateral, i.e., untreated hemisphere, with normal BBB, only 0.3 pmol MTX per mg brain was detected (Erdlenbruch *et al.*, 2003b). Even the penetration of high MW materials, such as albumin and antibodies, into the brain could be significantly increased (Erdlenbruch *et al.*, 2003a; Hülper *et al.*, 2011). The opening of the BBB *in vivo* was reversible and lasted for only a few minutes to about 1 h, depending on the AG concentration used (Erdlenbruch *et al.*, 2000; 2002). These properties would be advantageous in a clinical setting.

Results from *in vitro* and *in vivo* assays showed that AGs were non-toxic and that they were eliminated from the body through the kidneys (Erdlenbruch *et al.*, 2003b). Studies with radioactively labelled PG showed no enrichment in the brain or other organs (Erdlenbruch *et al.*, 2005). In freshly isolated brain capillaries, the marker dye fluorescein could diffuse into the capillary lumen after addition of AG. Using confocal microscopy, fluorescein could be found in the paracellular cleft, indicating an opening of the paracellular diffusion barrier (Erdlenbruch *et al.*, 2003a). However, the mode of action of AGs and their influence on BECs have not yet been elucidated.

The aim of the present work was to examine the direct short-term effects of AGs on cell viability and barrier properties in an *in vitro* model of the BBB, using cultures of BECs.

The integrity of the paracellular barrier of BECs was monitored following an acute treatment by AGs by the measurement of TEER and permeability for marker molecules (fluorescein and albumin), immunostaining for claudin-5 and β-catenin junctional proteins, and by the analysis of inter-endothelial tight junction strand complexity using freeze-fracture electron microscopy. The *trans*-interaction of claudin-5 was also examined to reveal the possible mode of action of AGs. Our *in vitro* data show for the first time that AGs reversibly enhanced the flux of molecules through brain endothelial cell monolayers, without causing fundamental alterations of the tight junction structure.

Methods

Animals

All animal care and experimental procedures complied with the recommendations of European Convention for the Protection of Vertebrate Animals Used for Experimental and other Scientific Purposes (Council Directive 86/609/EEC) and Hungarian National Law XXVIII./1998 and CLVIII./2011. on the protection of animals or the German National Law on the protection of animals (§ 4 Abs. 3) and were approved by the Animal Experimentation Committee of the Biological Research Centre, Hungarian Academy of Sciences (Hungary), and from the local Hungarian authorities (Permit numbers: XVI./03835/001/2006; XVI./834/2012) or the Animal Experimentation Committee of the Georg-August University Göttingen (reference no. T11/17). All studies involving animals are reported in accordance with the ARRIVE guidelines for reporting experiments involving animals (Kilkenny *et al.*, 2010; McGrath et al., 2010). A total of 70 animals were used in the experiments described here. Rats were kept in a controlled environment (22°C, 55% humidity, 12 h day-night rhythm) and had free access to standard diet and tap water.

Cell culture

Primary cultures of BECs were prepared from 2 week old outbred Wistar rats (Harlan Laboratories, Indianapolis, IN, USA) as described in detail by Veszelka *et al.*, (2007). Forebrains were collected in ice-cold sterile PBS; meninges were removed, grey matter was minced by scalpel into 1 mm^3 pieces and digested with 1 mg·mL^{-1} collagenase CLS2 (Worthington Biochem., Lakewood, NJ, USA) in DMEM for 1.5 h at 37°C. Microvessels were separated by centrifugation (1000× *g*, 20 min) in 20% BSA–DMEM from myelin containing elements and further digested with 1 mg·mL^{-1} collagenase–dispase (Roche, Basel, Switzerland) in DMEM for 1 h. Microvascular endothelial cell clusters were separated on a 33% continuous Percoll gradient (1000× *g*, 10 min), collected, and washed twice in DMEM before plating on collagen type IV and fibronectin-coated dishes, multiwell plates (Falcon, Becton Dickinson; Invitrogen, Carlsbad, CA, USA) or cell culture inserts (Transwell clear, 1 cm^2; pore size of 0.4 µm; Corning Costar Co., Lowell, MA, USA). Cultures were maintained in DMEM supplemented with 5 µg·mL^{-1} gentamicin, 20% plasma-derived bovine serum (First Link, Wolverhampton, UK), 1 ng·mL^{-1} basic fibroblast growth factor (Roche) and 100 µg·mL^{-1} heparin. During the first 2 days, culture medium

contained puromycin (4 µg·mL^{-1}) to selectively remove P-glycoprotein-negative contaminating cells (Perrière *et al.*, 2005). Cultures reached confluency within a week and were used for experiments. To induce BBB characteristics, BECs were co-cultured with rat cerebral glial cells (Deli *et al.*, 2005; Veszelka *et al.*, 2007).

Primary cultures of glial cells were prepared from 14 day old Wistar rats (Harlan Laboratories, Rossdorf, Germany or Charles River, Sulzfeld, Germany). Meninges were removed, and cortical pieces were mechanically dissociated in DMEM containing 5 µg·mL^{-1} gentamicin and 10% FBS and plated in poly-L-lysine-coated 12-well dishes and kept for a minimum of 3 weeks before use. In confluent glia cultures, 90% of cells were immunopositive for the astroglial cell marker glial fibrillary acidic protein, while the remaining 10% were immunopositive for CD11b, a marker of microglia.

For co-culture with BECs grown in cell culture, inserts were placed into multiwells containing astroglia at the bottom of the wells with endothelial culture medium in both compartments. When BECs became almost confluent, 550 nM hydrocortisone was added to the culture medium (Deli *et al.*, 2005). Before starting experiments, cells were treated with 8-(4-chlorophenylthio)-cAMP (CPT-cAMP; 250 µM) and Ro 20-1724 (17.5 µM; Roche) for 24 h to tighten junctions and elevate resistance (Deli *et al.*, 2005; Perrière *et al.*, 2005). All the experiments were performed with primary rat BEC cultures, except the claudin-claudin *trans*-interaction analyses which used HEK293 cells, as described below.

Treatments

AGs were tested on BECs at concentrations of 0–100 mM, with exposure for 5 min. The cells were incubated with AGs dissolved in DMEM culture medium to provide physiological conditions for the sensitive BEC monolayers. For viability studies, isotonic NaCl was used as in previous *in vivo* studies (Erdlenbruch *et al.*, 2003a,b; 2005). In all experiments, treatment solutions were added and removed from the cells very slowly and carefully not to disturb cell monolayers by the change of the medium.

Cell cytotoxicity assays for cell viability and apoptosis

Cell viability was determined by the WST-1 test which is based on the cleavage of a tetrazolium salt by mitochondrial dehydrogenases. About 5×10^3 BECs were seeded in flat-bottom, 96-well microtiter plates (100 µL per well), allowed to adhere for 24 h and then treated with increasing amounts of PG or HG for 5 min, then re-fed with culture medium. Cell viability was measured by adding 10 µL WST-1 reagent per well 45 min, 24 h, 48 h and 72 h after treatment. Two hours after addition of the WST-1 reagent, absorbance was determined by a SUNRISE microplate reader (TECAN, Crailsheim, Germany) at 450 nm with a reference filter at 690 nm. Cells treated with 1% Triton X-100 detergent (Tx-100) in serum-free medium for 6 h served as positive control, and untreated cells were used as reference.

Apoptosis was measured using a cell death detection ELISA kit (Roche Molecular Biochemicals, Mannheim, Germany). Cells were seeded in 96-well microtiter plates (200 µL per well). After 48 h, cells were treated with increasing amounts

of PG or HG for 5 min. As a positive control, cells were treated with 85 µM staurosporin for 1 h to induce apoptosis. DNA-histone complex provided with the kit also served as a technical control for the ELISA. The cytosolic fraction of treated or untreated cells was used as an antigen source in the sandwich ELISA. Incubation of the streptavidin-coated microplate with samples and the mixture of anti-histone–biotin and anti-DNA–peroxidase antibodies were performed according to the manufacturer's instructions. Absorption was measured by a SUNRISE microplate reader (TECAN) at 405 nm, with a reference filter at 492 nm.

Evaluation of the barrier integrity

TEER representing the permeability of tight junctions for sodium ions in culture conditions was measured by an EVOM resistance meter (World Precision Instruments Inc., Sarasota, FL, USA) using STX-2 electrodes, and expressed relative to the surface area of the endothelial monolayer ($\Omega \times cm^2$). The TEER of cell-free inserts (90–$100\ \Omega \times cm^2$) was subtracted from the experimental values. The TEER of rat primary BEC monolayers in co-culture varied between 250 and 400 $\Omega \times cm^2$, with a mean of $305(\pm 4)\ \Omega \times cm^2$ ($\pm$SEM; $n = 72$ experiments from three separate isolations.

The flux of sodium fluorescein (SF) and Evans blue-labelled albumin (EBA) across endothelial cell monolayers was determined as previously described (Veszelka et al., 2007). Cell culture inserts, following treatment and measurement of TEER, were transferred to 12-well plates containing 1.5 mL Ringer–HEPES solution (118 mM NaCl, 4.8 mM KCl, 2.5 mM CaCl$_2$, 1.2 mM MgSO$_4$, 5.5 mM D-glucose, 20 mM HEPES, pH 7.4) in the basolateral compartments. In apical chambers, culture medium was replaced by 500 µL Ringer–HEPES containing 10 µg·mL^{-1} SF (MW = 376 Da) and 165 µg·mL^{-1} EBA (Evans blue bound to 0.1% BSA; MW = 67 kDa). The inserts were transferred at 20, 40 and 60 min to a new well containing Ringer–Hepes solution. To minimize any unstirred water layers during permeability experiments, a horizontal shaker (Biosan, Riga, Latvia) was used at 100 r.p.m. The concentrations of the marker molecules in samples from the upper and lower compartments were determined with a microplate reader (EBA: absorbance at 620 nm; SF: excitation at 440 nm, emission at 525 nm; BMG Fluostar Optima; BMG Labtech, Ortenberg, Germany). Flux across cell-free inserts was also measured.

Transport was expressed as µL of donor (luminal) compartment volume from which the tracer is completely cleared. Transendothelial permeability coefficient (P_e) was calculated as previously described (Deli et al., 2005; Veszelka et al., 2007). Cleared volume was calculated from the concentration (C) of the tracer in the abluminal and luminal compartments and the volume (V) of the abluminal compartment (0.5 mL) by the following equation:

$$\text{Cleared volume (µL)} = \frac{C_{abluminal} \times V_{abluminal}}{C_{luminal}}$$

The average cleared volume was plotted against time, and permeability surface area product value for endothelial monolayer (PS_e) was calculated by the following formula:

$$\frac{1}{PS_{endothelial}} = \frac{1}{PS_{total}} - \frac{1}{PS_{insert}}$$

PS_e divided by the surface area (1 cm^2 for Transwell-12) generated the endothelial permeability coefficient in $10^{-6}\ cm·s^{-1}$. Mean P_e was $1.58 \pm 0.26 \times 10^{-6}\ cm·s^{-1}$ for SF and $0.15 \pm 0.07 \times 10^{-6}\ cm·s^{-1}$ for EBA ($n = 6$; two separate experiments).

Immunohistochemistry

Confluent BEC monolayers cultured on fibronectin- and collagen-coated inserts and treated with AGs and mannitol (1.4 M) were stained for claudin-5 (an integral membrane tight junction protein) and the adherens junction protein, β-catenin. The cultures were washed in PBS and fixed with ethanol (95 vol.%)–acetic acid (5 vol.%) for 10 min at –20°C. Cells were blocked with 3% (BSA)-PBS and incubated overnight with primary antibodies anti-claudin-5 (mouse monoclonal antibody; Zymed, South San Francisco, CA, USA) and anti-β-catenin (rabbit polyclonal antibody). Incubation with secondary antibodies Alexa Fluor-488-labelled anti-mouse IgG (Invitrogen), Cy3-labelled anti-rabbit IgG, and Hoechst dye 33342 to stain cell nuclei lasted for 1 h. Between incubations, cells were washed three times with PBS. Membranes were mounted in Gel Mount (Biomeda, Foster City, CA, USA) and staining was examined by a Nikon Eclipse TE2000 fluorescent microscope (Nikon, Tokyo, Japan) and photographed by a Spot RT digital camera (Diagnostic Instruments, Campbell, CA, USA).

Freeze-fracture electron microscopy

BECs grown on the fibronectin- and collagen-coated cell culture insert membrane were fixed with 2.5% glutaraldehyde in 0.1 M cacodylate buffer (pH 7.4) for 30 min at 4°C. After washing with cacodylate buffer several times, the membranes of the culture inserts were removed from their support and processed as previously described (Wolburg et al., 1994). In brief, small rectangles of the filters were incubated in 30% glycerol for 30 min, placed between two gold specimen holders, shock frozen in nitrogen slush (–210°C), and fractured at –150°C and 5×10^{-6} mbar (1 bar = 105 Pa) (freeze-fracturing apparatus BAF 400 D; BAL-TEC, Balzers, Liechtenstein). Fracture faces were immediately shadowed with platinum/carbon (2 nm, 45°) and carbon (20 nm, 90°) for stabilization. Replicas were cleaned with 12 % sodium hypochlorite, washed several times in double-distilled water and mounted on Pioloform-coated copper grids (Wacker Chemie, München, Germany). Replicas were analysed using a Zeiss EM10 electron microscope; electron micrographs were digitized and processed using Adobe Photoshop.

Analysis of claudin-5 trans-interaction

HEK293 cells stably transfected with murine claudin-5-yellow fluorescent protein (YFP) have been described previously (Piontek et al., 2008). Cells were maintained in DMEM supplemented with 10% fetal calf serum, 100 U·mL^{-1} penicillin, 100 µg·mL^{-1} streptomycin, 1% L-alanyl-L-glutamine (Invitrogen) and 0.5 mg·mL^{-1} G418 (Calbiochem, Darmstadt, Germany). To avoid clonal variations, pools containing different claudin-5-YFPs expressing and non-expressing colonies were used. Cells were plated on coverslips coated with poly-L-lysine (Sigma-Aldrich), 2 days later incubated with HG and the subcellular localization of claudin-5-YFPs in living cells was analysed by confocal microscopy. The integrity of the

plasma membrane of cells during the experiments was visualized by Trypan blue exclusion (Piontek *et al.*, 2008).

Data analysis

All data presented are means ± SEM. Data of WST-1 tests were calculated from triplicates, while data of cell death ELISA were calculated from six parallel wells and confirmed in three experiments. One-way ANOVA followed by Dunnett's multiple comparison test revealed statistically significant differences ($P < 0.05$) between treatment groups and NaCl-treated group. TEER data are from three independent experiments with triplicate samples. Statistical analysis was performed using two-way repeated measures ANOVA followed by Bonferroni post tests. The values measured in groups treated with PG, HG or mannitol were compared with the control value at each time point. Data of permeability for SF and EBA are from three independent experiments with triplicate samples. Statistical analysis was by one-way ANOVA followed by Newman–Keuls tests. The values measured after PG or HG treatment were compared with the permeability in control group.

Materials

All reagents were purchased from Sigma-Aldrich (St Louis, MO, USA), unless otherwise indicated. The short-chain AGs, 2-*O*-HG and 1-*O*-PG, were obtained from Genzyme Corporation (Cambridge, MA, USA). Both HG and PG are distributed in molecularly disperse form in aqueous solutions and do not form micelles in the applied concentrations (H. Eibl, personal communication.). To prepare isotonic stock solutions of AGs, 0.9% (w/v) NaCl solution and distilled water were used. Physiological osmolarity was determined.

Results

Cell viability assay

Toxicity of PG and HG on primary rat BECs was examined *in vitro* at different time points (Figure 1). To evaluate direct acute, as well as long-term, effects of 5 min incubation with different AG concentrations, on the viability of the cells, the WST-1 test was performed after 45 min, 24 h, 48 h and 72 h. Untreated cells were used as negative control and values from

Figure 1

The effect of short-time AG treatment on primary rat BECs. Increasing concentrations of PG and HG were used to study the cytotoxic effects on BECs. (A) WST-1 assay 45 min and 24 h after a 5 min AG treatment. Untreated cells served as negative control, cells treated with 1% Tx-100 for 6 h as positive control. For comparison, cells were treated with 0.7 and 1.4 M mannitol (M). All values presented are the means ± SEM, n = 3 for all groups. One-way ANOVA followed by Dunnett's multiple comparison test revealed statistically significant decrease (a) between treatment groups and NaCl-treated group. (B) Apoptosis ELISA 60 min after a 5 min AG treatment. Untreated cells served as negative control, DNA-histone complex served as positive control. All values presented are the means ± SEM, n = 6 for all groups. *P<0.05, significantly different from NaCl-treated group; one-way ANOVA followed by Dunnett's multiple comparison test.
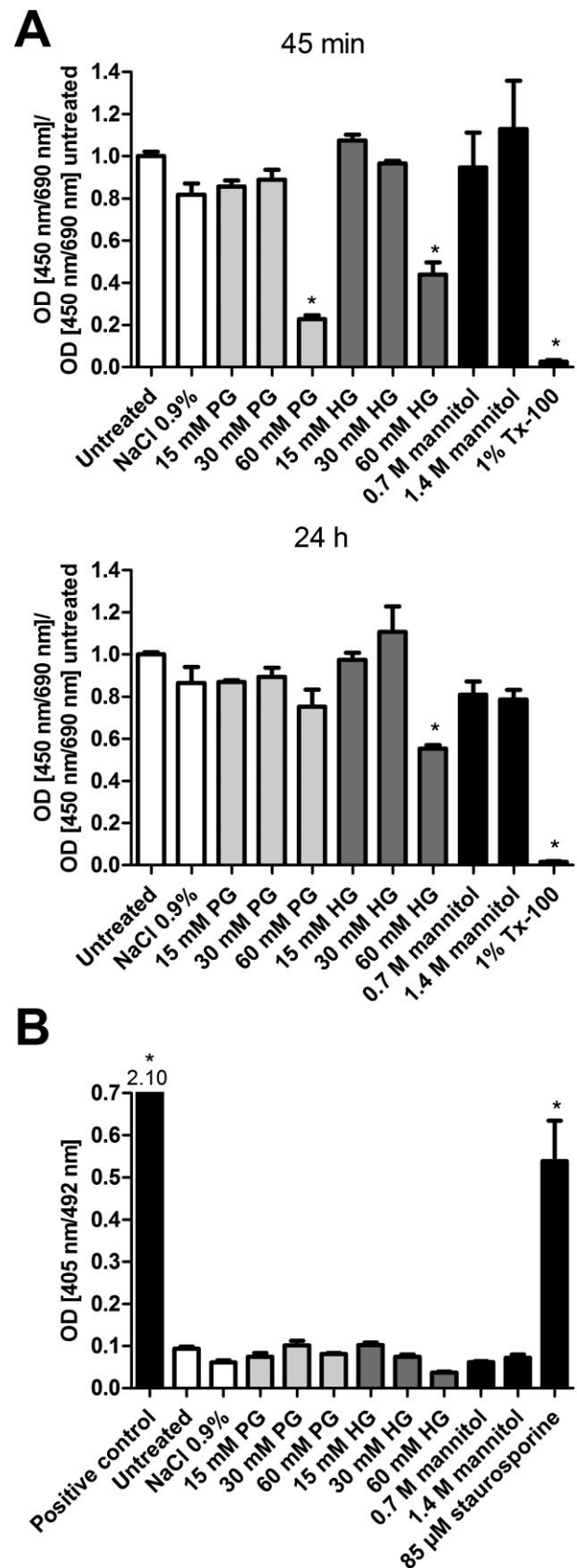
this control group were set to unity. The viability of cells treated with the detergent Tx-100 was drastically reduced, as expected. No toxic effect for PG or HG was detected up to 30 mM (Figure 1A). With higher concentrations of AGs, significant changes were measured both at 45 min ($P < 0.0001$, d.f. = 10, F = 16.09) and 24 h ($P < 0.0001$, d.f. = 10, F = 25.42) after the treatments (Figure 1A). PG at 60 mM concentration reduced viability significantly ($P < 0.01$) to about 23% of the control cells after 45 min, but endothelial cells were able to recover from this treatment within 24 h. Treatment with 60 mM HG resulted in a significant reduction ($P < 0.05$) of viability to 44% of the untreated cells after 45 min, but no recovery was seen within the next 24 h. The 5 min treatment period of the cells with 1.4 M mannitol did not lead to reduced viability. After 48 and 72 h, no further changes were observed, compared with the 24 h measurement (data not shown).

Assay for the induction of apoptosis

The induction of apoptosis after treatment of the cells with AGs was tested by an ELISA detecting cell death (Figure 1B). In addition to a positive control provided with the kit, staurosporin was used to induce apoptosis. Untreated cells served as negative control. No apoptosis could be detected in BECs treated with AGs (Figure 1B), while the positive controls differed significantly ($P < 0.001$) from the saline-treated negative control ($P < 0.0001$, d.f. = 11, F = 522.3). Similarly, treatment with AGs did not cause apoptosis in BECs after 24 h (data not shown).

Evaluation of barrier integrity: TEER and permeability measurements

To simulate the situation *in vivo*, i.e., AG treatment by a single bolus injection, the following experiments were performed, now using primary rat BECs co-cultured with glial cells, a relevant *in vitro* BBB model (Veszelka *et al.*, 2011). First, the direct and short-time effect of AGs on the ion flux through endothelial cell monolayers was analysed by TEER measurements (Figure 2). Only concentrations found non-toxic in the

viability experiments were used. TEER was quantified in untreated cells (negative control) and set to 100% at the beginning of the experiment (time –5 min). Cells were then incubated with different AGs for 5 min and further measurements were performed directly after removal of the test substance (0 min), as well as 10, 20 and 30 min after recovery in complete culture medium. Cells treated with 1.4 M mannitol served as positive controls. Significant changes in TEER were seen during the observation period both in PG-treated (column factor 79.26, $P < 0.0001$, d.f. = 3, F = 52.79; see Figure 2A) and HG-treated (column factor 97.71, $P < 0.0001$, d.f. = 3, F = 105.9; see Figure 2B) groups compared with the values measured in control group. Using 30 mM PG, TEER of BEC monolayers was reduced by 90% directly after termination of AG treatment (Figure 2A). After 10 min, TEER was 48% compared with untreated control suggesting recovery of the cells and the reversibility of the treatment with PG. The TEER of monolayers was further increased after 20 min of recovery. A lower 10 mM concentration of PG led to a 50% decrease of TEER directly after treatment and TEER also recovered over time. The effect of HG was also significant but less pronounced (Figure 2B). HG treatment at 30 and 10 mM concentrations resulted in TEER decrease by 58 and 29% compared with untreated cells measured directly after treatment. A complete recovery of barrier function was seen for both concentrations after 30 min. In contrast to these findings, TEER measured after 1.4 M mannitol treatment dropped below 25% of the control and remained there during the time frame of 30 min.

To complement TEER data, permeability of brain endothelial monolayers was measured with two test molecules, SF and EBA (Figure 3). Exposure of primary rat BECs to 30 mM PG or HG causing reversible changes in TEER, also led to a significantly increased flux of SF ($P = 0.0003$, d.f. = 3, F = 21.86 in case of PG, and $P = 0.0014$, d.f. = 3, F = 14.24 in case of HG; Figure 3A and B). After a recovery period of 15 min, permeability, values returned to the level of the control group again. In contrast to the results with the low MW SF (MW 376 Da), no significant increase in albumin (MW 67 kDa) permeability was observed in cell monolayers after treatment with
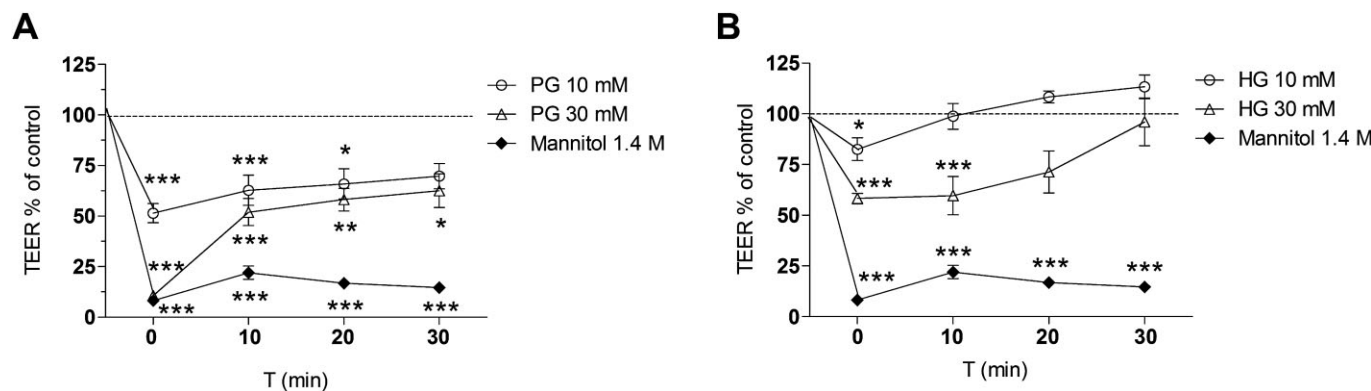

Figure 2

Changes in TEER were evaluated in primary rat brain endothelial cell monolayers treated with 10 and 30 mM PG (A), 10 and 30 mM HG (B), and mannitol (1.4 M) for 5 min. TEER was measured before treatment, directly after removal of AGs and mannitol (0 min), and following 10, 20 and 30 min of recovery in complete culture medium. All values presented are means ± SEM ($n = 3$). *$P < 0.05$, **$P < 0.01$, ***$P < 0.001$, significantly different from control group, at each time point; two-way repeated measures ANOVA followed by Bonferroni post test.
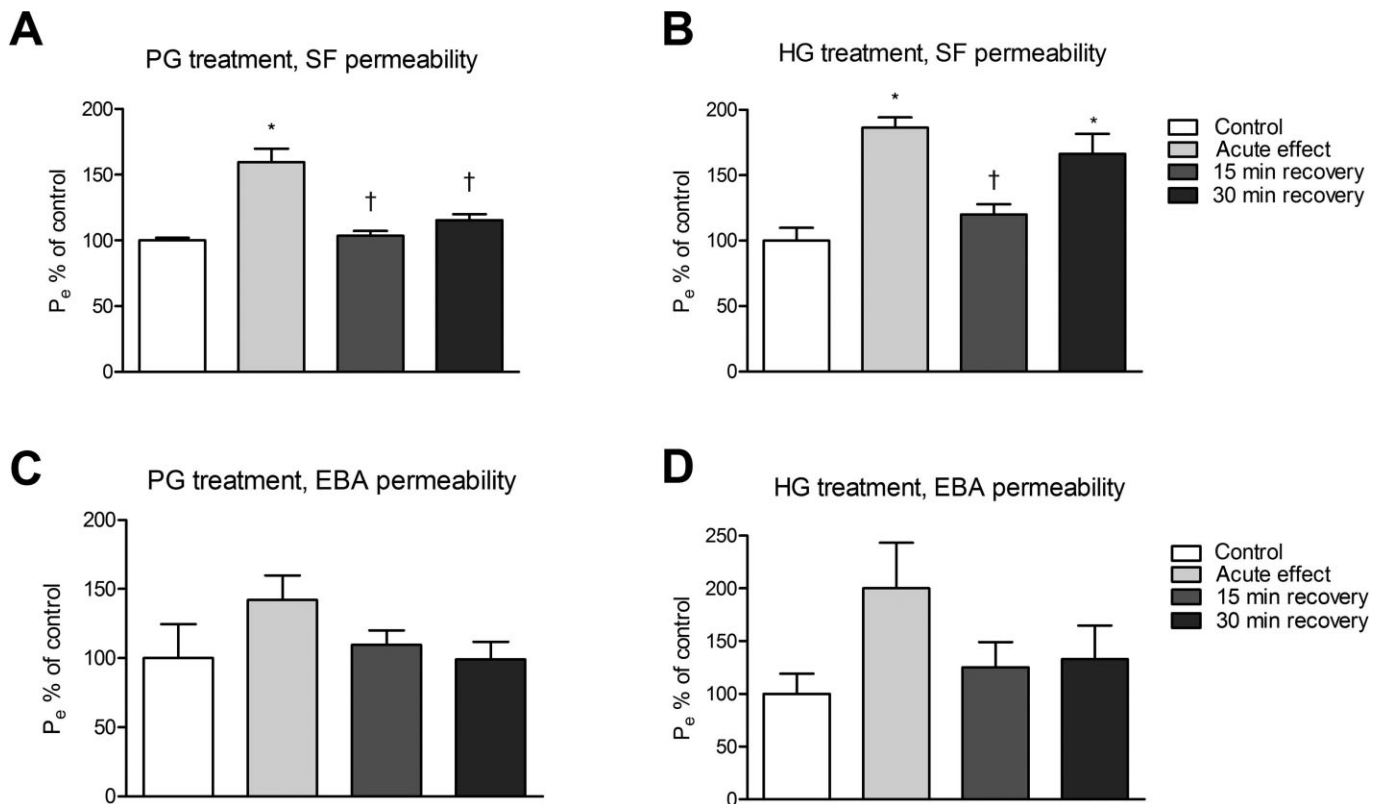
A
PG treatment, SF permeability

B
HG treatment, SF permeability

- □ Control
- ▨ Acute effect
- ▨ 15 min recovery
- ■ 30 min recovery

C
PG treatment, EBA permeability

D
HG treatment, EBA permeability

- □ Control
- ▨ Acute effect
- ▨ 15 min recovery
- ■ 30 min recovery

Figure 3

Changes in endothelial permeability (P_e) for the paracellular permeability marker SF (A, B) and the transendothelial permeability marker EBA (C, D) in primary rat brain endothelial cell monolayers treated with 30 mM of PG (A–C) or HG (B–D) for 5 min (acute effect). After removal of AGs, 15 and 30 min recovery was allowed in complete culture medium. P_e was calculated as described. Data are shown as percentage of control (means ± SEM; n = 3). *$P < 0.05$, significantly different from control group, †$P < 0.05$, significantly different from acute values; one-way ANOVA followed by Neuman–Keuls test.

30 mM HG (P = 0.2070, d.f. = 3, F = 1.907) or 30 mM PG (P = 0.3235, d.f. = 3, F = 1.356) (Figure 3C and D).

Immunohistochemistry for junctional proteins

Parallel to changes in barrier function, immunostaining for endothelium-specific integral fragmentation, cytoplasmic redistribution, and loss of both claudin-5 and β-catenin staining from the cell borders of primary rat BECs were visible directly after short-term PG, HG or mannitol treatment (Figure 4). After a recovery period of 15 or 30 min following HG or PG treatment, however, cells showed more prominent and clear immunostaining at the cell contacts compared with cells examined directly after treatment. In addition, a change in the shape of BECs after HG or mannitol exposure could be seen. Mannitol treatment caused monolayer disruption, holes became visible between BECs. In cells treated with hyperosmotic mannitol, perinuclear localization of β-catenin was also detectable.

Freeze-fracture electron microscopy of tight junction morphology

To investigate tight junction morphology and strand complexity, transmission electron microscopy was performed on freeze-fracture replicas from rat BECs of *in vitro* experiments fixed directly after incubation with 30 mM HG or 30 mM PG for 5 min or after a recovery period of 30 min (Figure 5). Untreated cells served as a control. The P-face/E-face ratio of tight junction strands was tested, which describes the relationship between the association of tight junction strands with the protoplasmic (P-face) and the external fracture face (E-face). The P-face/E-face ratio of tight junction strands has been suggested to be an important parameter for the functional quality of the barrier (Wolburg *et al*., 1994). Due to *cis*-interaction, claudin-5 monomers form oligomers in one membrane. *Trans*-interaction triggers the formation of polymeric discontinuous strands. During freeze fracturing, the claudin-5 oligomers slide out of the P-face and are seen on the exoplasmic E-face of the membrane as lines of particles. The number of P-face-associated tight junction particles was so low that it is difficult to recognize the tight junction network at the P-face (Figure 5). In contrast, at the E-face the tight junctions appear as pearl chain-like strands and are easily detectable. In our *in vitro* experiments, no changes in P-face/E-face association of the proteins in the fractures could be observed. In addition, no alterations of strand complexity between AG-treated and untreated control cells could be found (Figure 5).
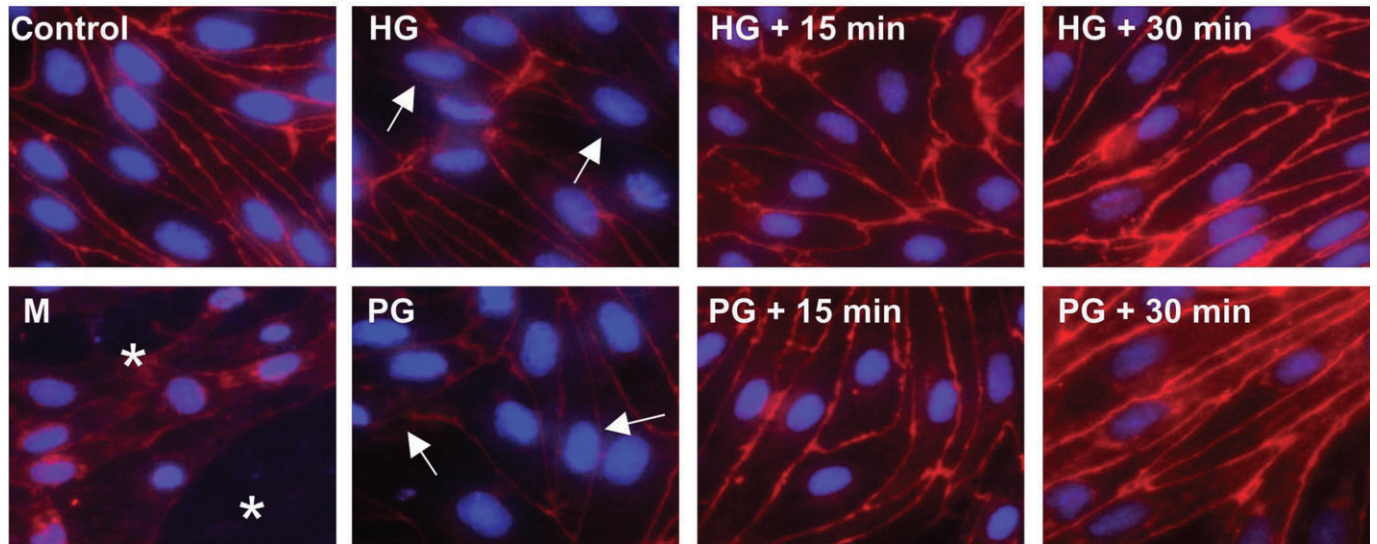
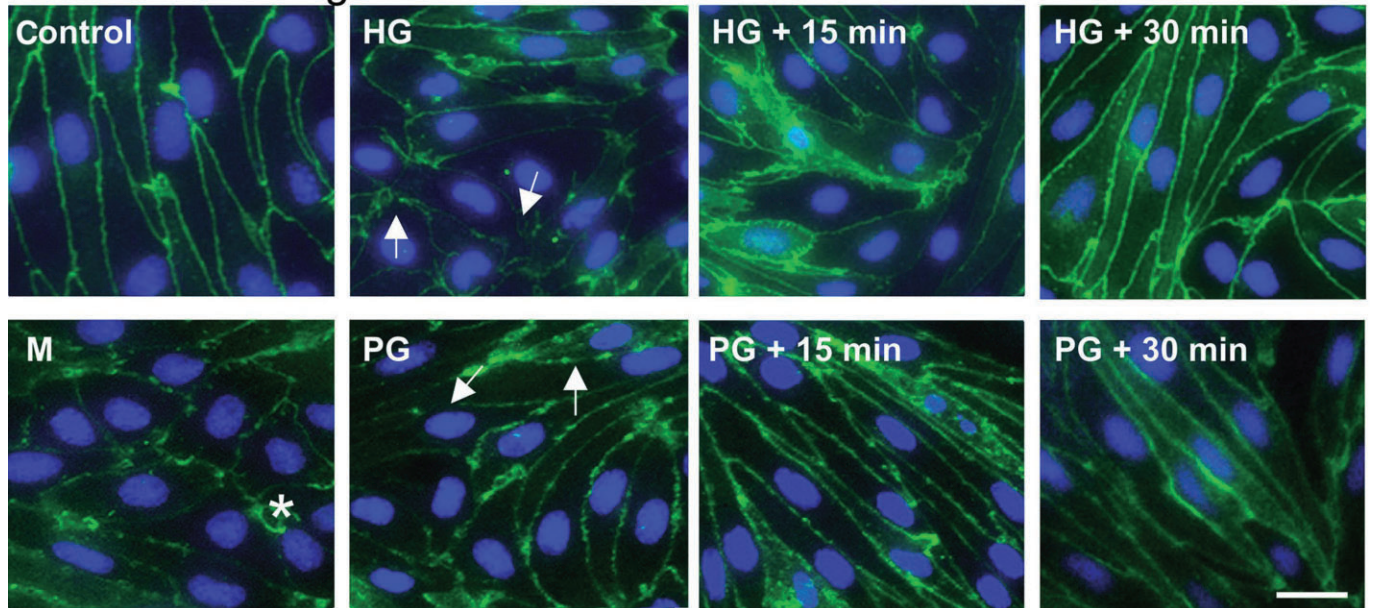## ß-catenin staining

Claudin-5 staining

Figure 4

Effect of AGs (30 mM) and mannitol (1.4 M) on immunostaining for claudin-5 and β-catenin junctional proteins in primary rat brain endothelial cells. Asterisks show holes formed between endothelial cells. Arrows indicate fragmentation, loss of junctional immunostaining, and cytoplasmic redistribution. Bar: 25 μm.

Analysis of claudin-5 trans-*interaction*

Finally, to further analyse the direct effect of AGs on claudin-5, which seals the intercellular cleft between adjacent cells by claudin-claudin *trans*-interaction, HEK293 cells stably transfected with YFP C-terminally tagged claudin-5 were treated with HG. In untreated cells, the claudins are mainly found in the plasma membrane between two transfected cells and the extracellular loops of the claudin molecules of the cell interact with those claudin loops of opposing cells by *trans*-interaction (Piontek *et al.*, 2008). This is reflected by a

strong enrichment of YFP at contacts between two claudin-5-YFP-expressing cells (Figure 6A). Treatment of these claudin-5-expressing HEK cells with 20 mM HG or 50 mM HG for 15 min had no visible effect on the YFP enrichment at cell-cell contacts, indicating no effect on claudin-5 *trans*-interaction (Figure 6B and C). Incubation with 100 mM HG for 15 min resulted in redistribution of claudin-5 (Figure 6D). The protein was not strongly enriched at contacts between two claudin-expressing cells but rather homogenously distributed throughout the plasma membrane. In addition,
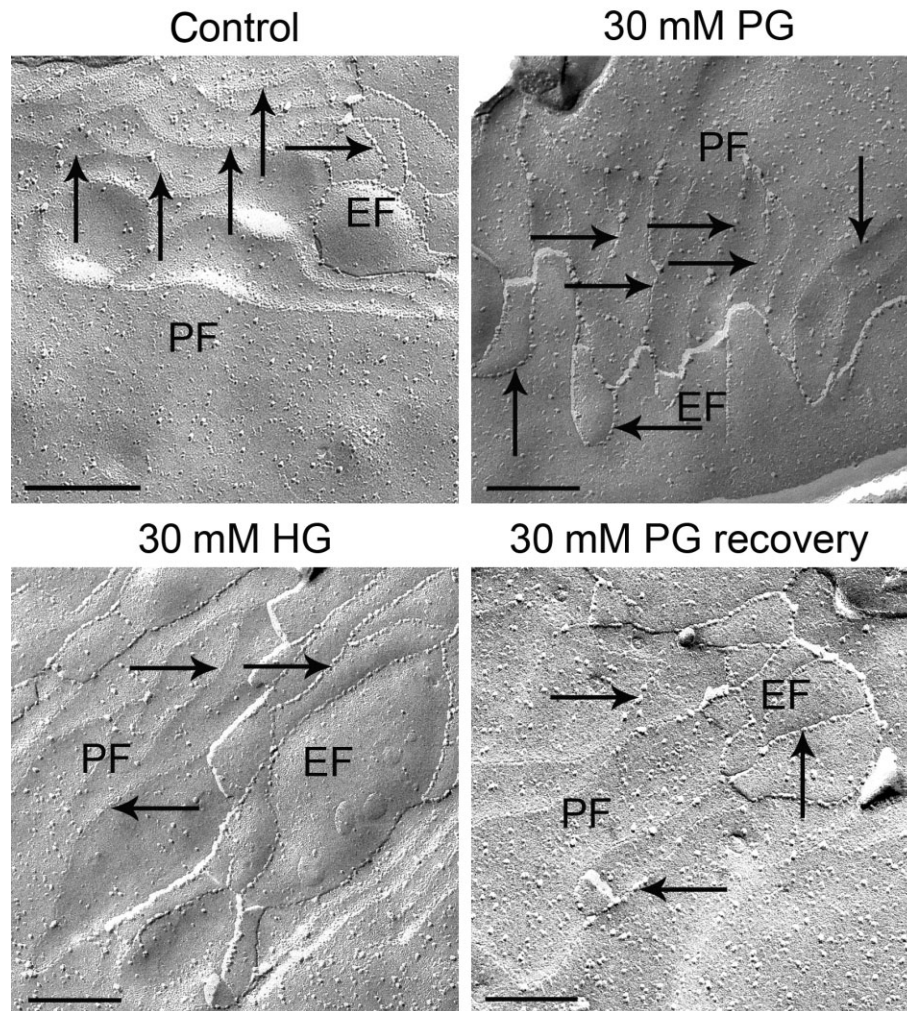
Control

30 mM PG

30 mM HG

30 mM PG recovery

Figure 5
Freeze-fracture analysis of the complexity and morphology of tight junction strands. Freeze-fracture replicas were prepared from cultured brain endothelial cells after PG or HG treatment. In all replicas tested, the tight junction strands were highly associated with the external fracture face (EF), only few particles were observed at the protoplasmic face (PF). Arrows point to EF or PF strands. Bar: 0.2 μm.

more claudin-5 was found in intracellular compartments (Figure 6D and E). However, this HG concentration caused leakage of the plasma membrane resulting in the entry of Trypan blue (red fluorescence in the cell cytoplasm; Figure 6D and E). It should be noted that the cellular response to HG was heterogeneous, as some cells with leakage of the plasma membrane and enrichment of claudin-5 were also found after incubation with high HG concentration (Figure 6E).

Discussion and conclusions

There are several different possible applications for AG-mediated BBB opening to increase the passage of drugs into the brain, including the treatment of primary brain tumours and the increasing number of cases with brain metastases. In this work, BBB opening and the reaction of BECs to AG exposure were studied in an *in vitro* model. *In vivo,*

PG and HG concentrations between 50 and 200 mM were used to open the BBB of rats and mice. The AGs were given as a single bolus injection into the internal carotid artery of rats and mice over 12–18 s, whereas the common carotid artery was clamped during the injection. In this system, opening of the BBB was dependent on the concentration of AG (Erdlenbruch *et al.*, 2000; 2003b), but it is not possible to predict the exact concentration and residence time of AG in brain capillaries. The primary cell co-culture BBB model (Veszelka *et al.*, 2007; 2011) was suitable to study the opening of the endothelial barrier with AGs *in vitro*. In contrast to the *in vivo* situation where the actual AG concentration needed for the barrier opening in an individual capillary is not known, in cultures every cell is exposed to the same AG concentration for the same time and detailed measurements under definite conditions can be performed. Compared with the initial *in vivo* conditions, the AG concentrations used *in vitro* were reduced from 50–100 mM to 10–30 mM, based on
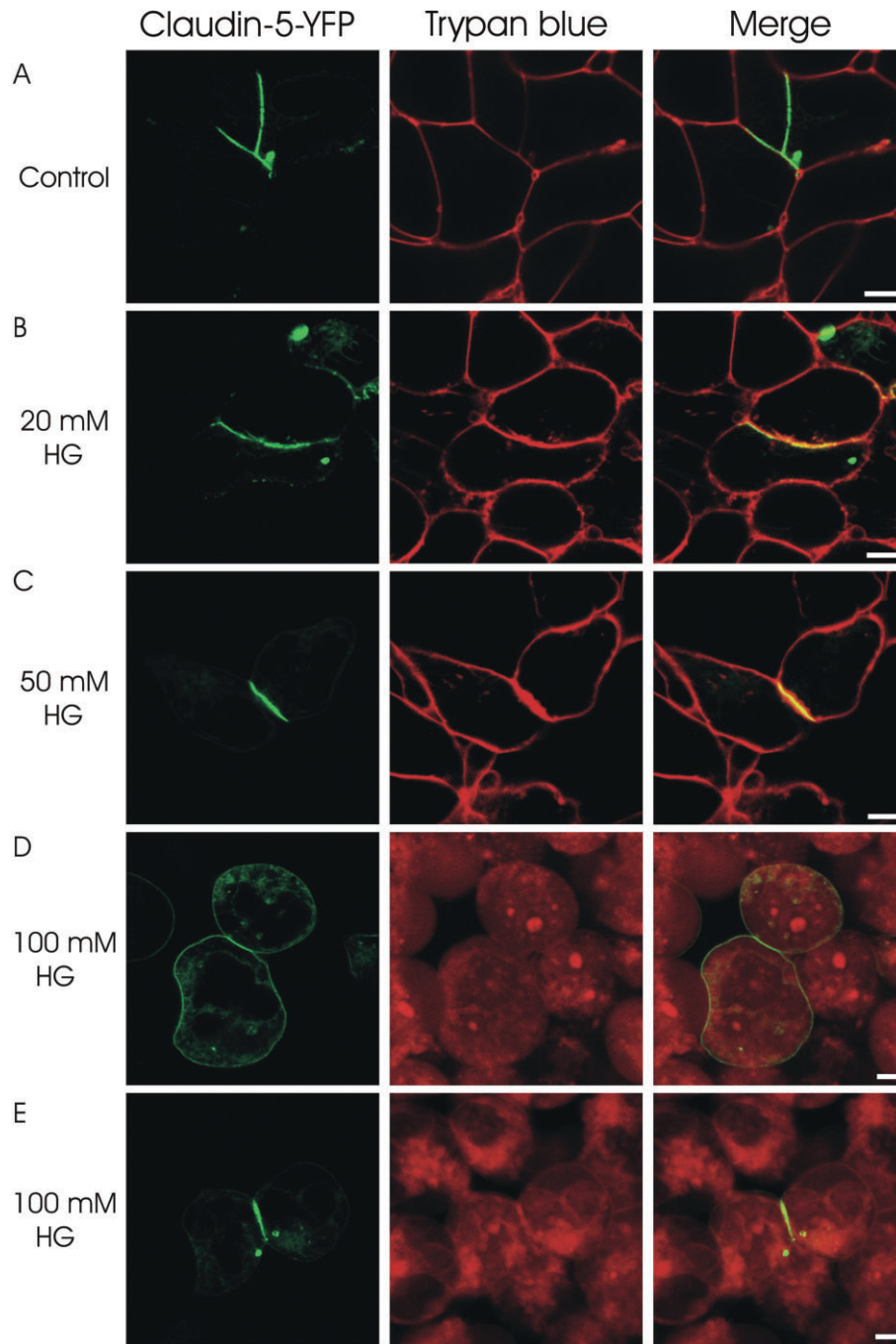
Figure 6

Analysis of claudin-claudin *trans*-interactions in HEK293 cells stably transfected with claudin 5-YFP (shown in green) by confocal fluorescence microscopy. Untreated cells show claudin-5 *trans*-interaction indicated by a strong enrichment of YFP at contacts between two claudin-5-YFP-expressing cells (A). 15 min treatment with 20 mM or 50 mM HG has no effect on claudin-5 *trans*-interaction (B + C). After 15 min treatment with 100 mM HG some cell pairs show loss of claudin-5 *trans*-interaction indicated by loss of contact enrichment (D) while other cell pairs still show contact enrichment (E). This high concentration causes damage to the plasma membrane of the cells, visible through Trypan blue (red fluorescence) entering the cells (D + E). Bar: 5 μm.

the results of the viability experiments and incubation time was increased from 18 s injection time to about 4.5 min. The permeability findings in this model are comparable to those of the *in vivo* experiments (Erdlenbruch *et al.*, 2005).

AG-mediated opening of the BBB was reflected by a decrease of TEER values. Comparable to the *in vivo* situation (Erdlenbruch *et al.*, 2003b), permeability of PG-treated BECs returned to control level after 15 min. PG treatment reduced

the TEER value of endothelial monolayers more effectively than HG treatment in the same concentration range. TEER decrease after treatment with AGs indicates that the paracellular diffusion barrier sealed by tight junctions was opened (Madara, 1998). The paracellular permeation is mainly restricted by integral membrane tight junction proteins, especially members of the claudin family (Krause *et al.*, 2008). They regulate the physiological paracellular permeability of ions and molecules smaller than 4 Å (Anderson and Van Itallie, 2009). In agreement with our present data, a decrease in TEER could also be observed after mannitol treatment in previous studies (Greenwood *et al.*, 1988; Farkas *et al.*, 2005).

Fluorescein is a small, water-soluble molecule; therefore, the increased passage of this dye across BEC monolayers after exposure of the cells to AGs indicates an opened paracellular pathway through tight junctions, similar to the changes in TEER. This is in agreement with the results from Erdlenbruch *et al.* (2003a). They incubated freshly isolated brain capillaries with AGs and fluorescein and observed fluorescein entering the lumen of the capillaries paracellularly. As observed for the TEER changes, the increased permeability for fluorescein was reversible.

In contrast to fluorescein, treatment with AGs did not result in statistically significant increase in albumin permeability in BECs despite a trend of elevation in albumin flux. Albumin passage is transcellular and is at a very low level at the BBB in physiological conditions *in vivo* (Abbott *et al.*, 2006). In pathological conditions, transport via this route is increased several fold, which can be independent from the opening of the paracellular pathway. A selective increase of vesicular albumin transport was demonstrated in cultured BECs during hypoxia (Plateel *et al.*, 1997). The paracellular pathway through intact tight junctions can also be opened for high MW compounds of the size of albumin (Artursson *et al.*, 1993; Knipp *et al.*, 1997). Changes in TEER, fluorescein and albumin flux all indicate that the major mechanism of the opening of the BBB by AGs could be a selective effect on the paracellular cleft and tight junctions between BECs. In addition to the observed functional alterations, immunostaining for claudin-5 and β-catenin in primary BECs also showed that junctions between the cells were affected after AG treatment. All these findings are in agreement with the data of Erdlenbruch *et al.* (2003a) who postulated that AGs increase mainly the paracellular route at the BBB.

The paracellular pathway can be altered by cytoskeletal disruption (Bruewer *et al.*, 2004; Ivanov *et al.*, 2005) and the tightness of tight junctions seems to be controlled by cytoskeletal dynamics (Lai *et al.*, 2005; Hartsock and Nelson, 2008). β-Catenin is an adherens junction protein, linking the integral membrane junctional proteins to the cytoskeleton (Noda *et al.*, 2010). The observed changes in the shape of BECs after AG exposure might be an indication for the involvement of actin-junctional anchoring in the mechanism of AGs.

Bearing this observation and possible cytoskeletal changes in mind, it was possible that AGs altered the morphology or complexity of tight junction strands leading to increased paracellular permeability. Tight junction strands are crucial in the regulation of the paracellular route in BECs (Wolburg *et al.*, 1994; Rubin and Staddon, 1999). Wolburg *et al.* (1994) described that a higher amount of P-face-

associated tight junction strands can be observed in BECs as compared with non-BECs, and 16–24 h of cultivation led to a massive loss of P-face association of these tight junction strands. This was interpreted as the ability of the brain microenvironment to induce and maintain a high P-face association of tight junction strands. In order to imitate the brain microenvironment, endothelial cells were treated with forskolin for 2 days, which resulted in an increase of P-face association and complexity of tight junctions (Wolburg *et al.*, 1994). In the present study, cell cultures were treated with AGs for only 5 min, but this very brief treatment caused a significant change in paracellular permeability measured by functional assays. In contrast, junction morphology, including both complexity and E/P-face association of the tight junctions, between control and AG-treated BECs, was not altered. In the control and in the treated samples, at the E-face, the tight junctions appeared as pearl chain-like strands. According to our results, the functional changes elicited by AGs were not accompanied by structural alterations on the electron microscopic level. Therefore, the frequently asked question whether or not functional changes of the barrier would always go in parallel with strand alterations must be answered, at least under *in vitro* conditions, with 'no'. This finding is supported by a recent observation that regulation of the barrier permeability can not only be achieved by structural rearrangement of the tight junction strands but it can occur without any morphologically visible changes (Piehl *et al.*, 2010). Tight junctions are able to change functionally very quickly through phosphorylation. Reduced permeability can be seen as soon as 10 min after cAMP treatment in cultured BECs (Deli *et al.*, 1995) and turnover of tight junction proteins is also rapid, for example, the membrane half-life of claudin-5 is 33 s (Piontek *et al.*, 2011).

Claudin-5 is a major tight junction protein in BECs, closing the intercellular cleft by interaction of its extracellular loops with the corresponding loops of claudins of the adjacent endothelial cell (see Krause *et al.*, 2009). HEK293 cells expressing fluorescent claudin-5 show homophilic claudin *trans*-interaction by cell-contact enrichment independent of ZO-1 or cytoskeleton anchorage (Piontek *et al.*, 2008). The direct influence of AGs on such claudin *trans*-interactions was tested on this model. We found that the *trans*-interaction of claudin-5 was unchanged by HG in non-toxic concentrations used for functional tests of paracellular permeability. Only the highest concentration of HG modified the membrane localization and *trans*-interaction of claudin-5 which at the same time led to membrane destruction and was also toxic in other tests. This indicates that the effects of AGs on the plasma membrane of cells may be greater than direct effects on claudin-5 *trans*-interaction. In BECs treated with AGs, the intensity of immunostaining for claudin-5 decreased at the cell borders but increased in the cytoplasm, indicating a redistribution of the tight junction protein. These data demonstrate that claudin interactions might not be affected directly by AGs, and some other mechanisms involving cytoskeleton anchorage of claudins could mediate the effect.

Biologically active lipids, like the arachidonic acid metabolite prostanoids and leukotrienes, influence BBB permeability. Recently, a prostanoid EP₁ receptor antagonist was shown to prevent BBB leakage after cerebral ischaemia (Fukumoto *et al.*, 2010). Although this field is experimentally

unexplored, the effect of short-chain AGs on the BBB via lipid receptors cannot be ruled out. Modification of lipid composition and/or fluidity of rafts containing integral membrane tight junction proteins (Dodelet-Devillers *et al*., 2009) could be another way for AGs to selectively modify the tight junctions of brain endothelial cell monolayers. Further investigations are needed to elucidate which molecules are involved in the opening of the paracellular transport route by AGs.

Taken together, the results of our study demonstrated, for the first time, that a brief treatment of cultured BECs with short-chain AGs at non-toxic concentrations reversibly opens the paracellular barrier without long-lasting impairment. The increase in the penetration rate of water-soluble molecules across BECs was not accompanied by changes in tight junction strand complexity. These *in vitro* observations demonstrate that recovery of the monolayer integrity after AG treatment is possible and exposure to AGs does not lead to destruction of BBB functions and morphology. The study confirms the results of previous *in vivo* experiments on rats and mice and suggests that the properties of AGs may be suitable for opening the BBB to treat brain malignancies.

Acknowledgements

Conflict of interest

There is no conflict of interest for any of the authors.

References

Abbott NJ, Rönnbäck L, Hansson E (2006). Astrocyte-endothelial interactions at the blood-brain barrier. Nat Rev Neurosci 7: 41–53.

Anderson JM, Van Itallie CM (2009). Physiology and function of the tight junction. Cold Spring Harb Perspect Biol 1: a002584.

Artursson P, Ungell AL, Löfroth JE (1993). Selective paracellular permeability in two models of intestinal absorption: cultured monolayers of human intestinal epithelial cells and rat intestinal segments. Pharm Res 10: 1123–1129.

Blasig IE, Winkler L, Lassowski B, Mueller SL, Zuleger N, Krause E *et al*. (2006). On the self-association potential of transmembrane tight junction proteins. Cell Mol Life Sci 63: 505–514.

Bruewer M, Hopkins AM, Hobert ME, Nusrat A, Madara JL (2004). RhoA, Rac1, and Cdc42 exert distinct effects on epithelial barrier via selective structural and biochemical modulation of junctional proteins and F-actin. Am J Physiol Cell Physiol 287: C327–C335.

Dejana E, Orsenigo F, Lampugnani MG (2008). The role of adherens junctions and VE-cadherin in the control of vascular permeability. J Cell Sci 121: 2115–2122.

Deli MA (2009). Potential use of tight junction modulators to reversibly open membranous barriers and improve drug delivery. Biochim Biophys Acta 1788: 892–910.

Deli MA (2011). Drug transport and the blood-brain barrier. In: Tihanyi K, Vastag M (eds). Solubility, Delivery, and ADME Problems of Drugs and Drug-Candidates. Washington: Bentham Science Publ. Ltd., pp. 144–165.

Deli MA, Dehouck MP, Ábrahám CS, Cecchelli R, Joó F (1995). Penetration of small molecular weight substances through cultured bovine brain capillary endothelial cell monolayers: the early effects of cyclic adenosine 3',5'-monophosphate. Exp Physiol 80: 675–678.

Deli MA, Ábrahám CS, Kataoka Y, Niwa M (2005). Permeability studies on in vitro blood-brain barrier models: physiology, pathology, and pharmacology. Cell Mol Neurobiol 25: 59–127.

Demeule M, Regina A, Che C, Poirier J, Nguyen T, Gabathuler R *et al*. (2008). Identification and design of peptides as a new drug delivery system for the brain. J Pharmacol Exp Ther 324: 1064–1072.

Dhanikula RS, Argaw A, Bouchard JF, Hildgen P (2008). Methotrexate loaded polyether-copolyester dendrimers for the treatment of gliomas: enhanced efficacy and intratumoral transport capability. Mol Pharm 5: 105–116.

Dodelet-Devillers A, Cayrol R, van Horssen J, Haqqani AS, de Vries HE, Engelhardt B *et al*. (2009). Functions of lipid raft membrane microdomains at the blood-brain barrier. J Mol Med (Berl) 87: 765–774.

Doolittle ND, Miner ME, Hall WA, Siegal T, Jerome E, Osztie E *et al*. (2000). Safety and efficacy of a multicenter study using intraarterial chemotherapy in conjunction with osmotic opening of the blood-brain barrier for the treatment of patients with malignant brain tumors. Cancer 88: 637–647.

Erdlenbruch B, Jendrossek V, Eibl H, Lakomek M (2000). Transient and controllable opening of the blood-brain barrier to cytostatic and antibiotic agents by alkylglycerols in rats. Exp Brain Res 135: 417–422.

Erdlenbruch B, Jendrossek V, Kugler W, Eibl H, Lakomek M (2002). Increased delivery of erucylphosphocholine to C6 gliomas by chemical opening of the blood-brain barrier using intracarotid pentylglycerol in rats. Cancer Chemother Pharmacol 50: 299–304.

Erdlenbruch B, Alipour M, Fricker G, Miller DS, Kugler W, Eibl H *et al*. (2003a). Opening of the blood-brain barrier to small and large fluorescence markers in normal and C6 glioma bearing rats and isolated capillaries using intracarotid short chain alkylglycerols. Br J Pharmacol 140: 1201–1210.

Erdlenbruch B, Schinkhof C, Kugler W, Heinemann DEH, Herms J, Eibl H *et al*. (2003b). Intraarterial short chain alkylglycerols for increased delivery of methotrexate to the rat brain. Br J Pharmacol 139: 685–694.

Erdlenbruch B, Kugler W, Schinkhof C, Neurath H, Eibl H, Lakomek M (2005). Blood-brain barrier opening with alkylglycerols: biodistribution of 1-O-pentylglycerol after intravenous and intracarotid administration in rats. J Drug Target 13: 143–150.

Farkas A, Szatmári E, Orbók A, Wilhelm I, Wejksza K, Nagyőszi P *et al*. (2005). Hyperosmotic mannitol induces Src kinase-dependent phosphorylation of beta-catenin in cerebral endothelial cells. J Neurosci Res 80: 855–861.

Fellner F, Bauer B, Miller DS, Schaffrik M, Fankhänel M, Spruß T *et al*. (2002). Transport of paclitaxel (Taxol) across the blood-brain barrier in vitro and in vivo. J Clin Invest 110: 1309–1318.

Fukumoto K, Takagi N, Yamamoto R, Moriyama Y, Takeo S, Tanonaka K (2010). Prostanoid EP1 receptor antagonist reduces blood-brain barrier leakage after cerebral ischemia. Eur J Pharmacol 640: 82–86.

Furuse M, Sasaki H, Fujimoto K, Tsukita S (1998). A single gene product, claudin-1 or -2, reconstitutes tight junction strands and recruits occludin in fibroblasts. J Cell Biol 143: 391–401.

Golden PL, Pollack GM (2003). Blood-brain barrier efflux transport. J Pharm Sci 92: 1739–1753.

Greenwood J, Luthert PJ, Pratt OE, Lantos PL (1988). Hyperosmolar opening of the blood-brain barrier in the energy-depleted rat brain. Part 1. Permeability studies. J Cereb Blood Flow Metab 8: 9–15.

Hartsock A, Nelson WJ (2008). Adherens and tight junctions: structure, function and connections to the actin cytoskeleton. Biochim Biophys Acta 1778: 660–669.

Hülper P, Dullin C, Kugler W, Lakomek M, Erdlenbruch B (2011). Monitoring proteins using in vivo near-infrared time-domain optical imaging after 2-O-hexyldiglycerol-mediated transfer to the brain. Mol Imaging Biol 13: 275–283.

Ivanov AI, Hunt D, Utech M, Nusrat A, Parkos CA (2005). Differential roles for actin polymerization and a myosin II motor in assembly of the epithelial apical junctional complex. Mol Biol Cell 16: 2636–2650.

Kemper EM, Boogerd W, Thuis E, Beijnen JH, van Tellingen O (2004). Modulation of the blood-brain barrier in oncology: therapeutic opportunities for the treatment of brain tumors. Cancer Treat Rev 30: 415–423.

Knipp GT, Ho NF, Barsuhn CL, Borchardt RT (1997). Paracellular diffusion in Caco-2 cell monolayers: effect of perturbation on the transport of hydrophilic compounds that vary in charge and size. J Pharm Sci 86: 1105–1110.

Krause G, Winkler L, Mueller SL, Haseloff RF, Piontek J, Blasig IE (2008). Structure and function of claudins. Biochim Biophys Acta 1778: 631–645.

Krause G, Winkler L, Piehl C, Blasig I, Piontek J, Müller SL (2009). Structure and function of extracellular claudin domains. Ann N Y Acad Sci 1165: 34–43.

Lai CH, Kuo KH, Leo JM (2005). Critical role of actin in modulating BBB permeability. Brain Res Brain Res Rev 50: 7–13.

Madara JL (1998). Regulation of the movement of solutes across tight junctions. Annu Rev Physiol 60: 143–159.

Neuwelt EA, Barnett PA, McCormick CI, Frenkel EP, Minna JD (1985). Osmotic blood-brain barrier modification: monoclonal antibody, albumin, and methotrexate delivery to cerebrospinal fluid and brain. Neurosurgery 17: 419–423.

Noda K, Zhang J, Fukuhara S, Kunimoto S, Yoshimura M, Mochizuki N (2010). Vascular endothelial-cadherin stabilizes at cell-cell junctions by anchoring to circumferential actin bundles through alpha- and beta-catenins in cyclic AMP-Epac-Rap1 signal-activated endothelial cells. Mol Biol Cell 21: 584–596.

O'Brien FE, Clarke G, Fitzgerald P, Dinan TG, Griffin BT, Cryan JF (2012). Inhibition of P-glycoprotein enhances transport of imipramine across the blood–brain barrier: microdialysis studies in conscious freely moving rats. Br J Pharmacol 166: 1333–1343.

Pardridge WM (2002). Drug and gene targeting to brain with molecular Trojan horses. Nat Rev Drug Discov 1: 131–139.

Perrière N, Demeuse PH, Garcia E, Regina A, Debray M, Andreux JP et al. (2005). Puromycin-based purification of rat brain capillary endothelial cell cultures. Effect on the expression of blood-brain barrier-specific properties. J Neurochem 93: 279–289.

Piehl C, Piontek J, Cording J, Wolburg H, Blasig IE (2010). Participation of the second extracellular loop of claudin-5 in paracellular tightening against ions, small and large molecules. Cell Mol Life Sci 67: 2131–2140.

Piontek J, Winkler L, Wolburg H, Müller SL, Zuleger N, Piehl C et al. (2008). Formation of tight junction: determinants of homophilic interaction between classic claudins. FASEB J 22: 146–158.

Piontek J, Fritzsche S, Cording JD, Richter S, Hartwig J, Walter M et al. (2011). Elucidating the principles of the molecular organization of heteropolymeric tight junction strands. Cell Mol Life Sci 68: 3903–3918.

Plateel M, Teissier E, Cecchelli R (1997). Hypoxia dramatically increases the nonspecific transport of blood-borne proteins to the brain. J Neurochem 68: 874–877.

Rapoport SI (2000). Osmotic opening of the blood–brain barrier: principles, mechanisms, and therapeutic applications. Cell Mol Neurobiol 20: 217–230.

Reardon DA, Rich JN, Friedman HS, Bigner DD (2006). Recent advances in the treatment of malignant astrocytoma. J Clin Oncol 24: 1253–1265.

Reese TS, Karnovsky MJ (1967). Fine structural localization of a blood-brain barrier to exogenous peroxidase. J Cell Biol 34: 207–217.

Rubin LL, Staddon JM (1999). The cell biology of the blood-brain barrier. Annu Rev Neurosci 22: 11–28.

Siegal T, Rubinstein R, Bokstein F, Schwartz A, Lossos A, Shalom E et al. (2000). In vivo assessment of the window of barrier opening after osmotic blood – brain barrier disruption in humans. J Neurosurg 92: 599–605.

Taddei A, Giampietro C, Conti A, Orsenigo F, Breviario F, Pirazzoli V et al. (2008). Endothelial adherens junctions control tight junctions by VE-cadherin-mediated upregulation of claudin-5. Nat Cell Biol 10: 923–934.

Unger C, Eibl H, von Heyden HW, Kirsch B, Nagel GA (1985). Blut-Hirn-Schranke und Penetration von Zytostatika. Klin Wochenschr 63: 565–571.

Veszelka S, Pásztói M, Farkas AE, Krizbai I, Ngo TK, Niwa M et al. (2007). Pentosan polysulfate protects brain endothelial cells against bacterial lipopolysaccharide-induced damages. Neurochem Int 50: 219–228.

Veszelka S, Kittel A, Deli MA (2011). Tools of modelling blood-brain barrier penetrability. In: Tihanyi K, Vastag M (eds). Solubility, Delivery, and ADME Problems of Drugs and Drug-Candidates. Washington: Bentham Science Publ. Ltd., pp. 144–165.

van Vliet EA, Zibell G, Pekcec A, Schlichtiger J, Edelbroek PM, Holtman L et al. (2010). COX-2 inhibition controls P-glycoprotein expression and promotes brain delivery of phenytoin in chronic epileptic rats. Neuropharmacology 58: 404–412.

Wolburg H, Neuhaus J, Kniesel U, Krauss B, Schmid EM, Öcalan M (1994). Modulation of tight junction structure in blood-brain barrier endothelial cells. Effects of tissue culture, second messengers and cocultured astrocytes. J Cell Sci 107: 1347–1357.